Hyperaccuracy Three-dimensional Reconstruction Is Able to Maximize the Efficacy of Selective Clamping During Robot-assisted Partial Nephrectomy for Complex Renal Masses

(Article begins on next page)

19 May 2024

Hyperaccuracy Three-dimensional Reconstruction Is Able to Maximize the Efficacy of Selective Clamping During Robot-assisted Partial Nephrectomy for Complex Renal Masses

Francesco Porpiglia *, Cristian Fiori, Enrico Checcucci, Daniele Amparore, Riccardo Bertolo

Division of Urology, University of Turin, San Luigi Gonzaga Hospital, Orbassano (Turin), Italy

* Corresponding author. Division of Urology, Department of Oncology, School of Medicine, University of Turin, San Luigi Gonzaga Hospital, Regione Gonzole 10, 10043 Orbassano (Turin), Italy. Tel. +390119026558; Fax: +390119038654.
E-mail address: porpiglia@libero.it (F. Porpiglia).

Abstract

Background: Available technologies could avoid global ischemia for the removal of a renal tumor.

Objective: To present hyperaccuracy three-dimensional (HA3D) reconstruction during robot-assisted partial nephrectomy (RAPN) and compare its efficacy in sponsoring successful selective clamping of renal arterial branches during RAPN.

Design, setting, and participants: Patients undergoing RAPN (January 2016–July 2017) for renal mass PADUA score ≥10 who underwent abdominal computed tomography scan with angiography. Since February 2017 HA3D reconstruction was performed.

Surgical procedure: HA3D reconstruction-aided RAPN and standard RAPN with selective clamping.

Measurements: Intraoperative variables focusing on the renal arterial pedicle management and success rate of its planned management.

Results and limitations: Thirty-one patients in group no HA3D and 21 in group HA3D. The median (standard deviation) tumor size was 50.9 and 50.8 mm ($p = 0.97$), and median PADUA scores 10.5 and 11 ($p = 0.85$) for groups no HA3D and HA3D, respectively. In group no HA3D, a significantly higher number of patients underwent global ischemia (80% vs 24%, $p < 0.01$). Of note, in 90% of the group HA3D cases, intraoperative management of the renal pedicle was performed as preoperatively planned; in 39% of the group no HA3D cases, management of the renal arterial pedicle was varied intraoperatively ($p = 0.04$). We disclose the limited sample size and the experimental technique.

Conclusions: Preoperative simulation of selective ischemia was feasible and effective with HA3D reconstruction. In all the RAPN cases performed, selective clamping was successful, avoiding ischemia of the healthy renal remnant. A strict collaboration between urologists and bioengineers is mandatory to improve the technology.

Patient summary: In this report, we found that an accurate three-dimensional reconstruction of the kidney before conservative surgery for renal cancer seems to help in avoiding the global ischemia of the kidney. Further studies are needed to conclude if avoiding a percentage of ischemia to the kidney is clinically relevant.

1. Introduction

Among modifiable factors influencing renal function after partial nephrectomy (PN), recent reports indicated that the quantity of the preserved renal parenchyma after PN is one of the most important predictors of long-term renal function [1–4]. Conversely, we still miss strong evidence about renal ischemia [5–7]. By identifying the unique blood supply of the resectable renal mass, global

ischemia to the healthy remnant may be avoided. With this aim, several techniques of selective/superselective renal ischemia were described [8–11]. Interestingly, studies investigating their benefit on the renal functional outcome did not reveal clinically significant difference with global ischemia [12–14]. With the latest technological innovations we have entered the ""precision surgery" era [15]. Given the technologies available, if renal ischemia is among the factors influencing renal damage, it would be theoretically intolerable that the removal of a renal tumor requires global ischemia. Detailed understanding of the surgical anatomy of the kidney is mandatory. This is undoubtedly not possible by solely using two-dimensional computed tomography (CT)-scan slices. Fluorescence guidance was introduced as a sponsor of selective clamping, but it has not gained widespread distribution due to being an empirical technique with a high percentage of failures [11,12,16]. Development of a precise radiological guidance technology addressed to this issue would be a superior technique [17,18]. After a promising beginning [19], trying to contribute to this field, we began our experience with the software authorized for medical use specific for hyperaccuracy three-dimensional (HA3D) reconstruction of the anatomical structures from CT-scan images. The primary aim of this study was to evaluate the reliability of the software in reproducing the in vivo anatomical structures of the kidney visualized during robot-assisted PN (RAPN). The secondary aim of this study was to compare the management of renal pedicle after RAPN was performed with preoperative planning based on HA3D reconstruction with that during RAPN with standard preoperative planning based on bidimensional CT-scan slices.

2. Patients and methods

Eligible study patients signed a written informed consent form approved by the Institutional Ethics Committee (IRB approval 106/2011). We prospectively enrolled patients who underwent RAPN between January 1, 2016 and July 31, 2017. All patients underwent abdominal CT scan with angiography. Specifically for the purpose of this study, since February 1, 2017, prior to the

intervention, the patients were addressed to undergo high-resolution abdominal CT scan with HA3D reconstruction.

2.1. Inclusion/exclusion criteria

We enrolled all the patients with complex renal tumors (PADUA score ≥10) who were candidate to RAPN, with baseline estimated glomerular filtration rate (according to the Modification of Diet in Renal Disease Study formula) of >60 ml/min [20] (stage I/II chronic kidney disease according to the Kidney Disease Outcomes Quality Initiative). Patients with a solitary or horseshoe-shaped kidney at the preoperative CT scan were excluded.

2.2. Intervention

All patients underwent transperitoneal RAPN performed by a single surgeon with expertise in minimally invasive renal surgery (>500 procedures carried out). The arterial renal pedicle was dissected on the basis of the CT-scan bidimensional images. In patients who underwent HA3D reconstruction, renal pedicle management and subsequent ischemia were simulated on the created virtual model (Fig. 1), then the dissection of the pedicle was guided by HA3D reconstruction on the tablet next to the console, manually oriented by the assistant, according to the in vivo anatomy. From the main artery, dissection was carried on following the renal branches as anticipated by HA3D reconstruction. The dissection of renal pedicle ended with the identification of the branch/branches of renal artery supplying the tumor (Fig. 2). The branch/branches of the renal artery contacting the tumor at HA3D reconstruction and confirmed in the in vivo anatomy were clamped by bulldog. In some cases, identification of the tumor feeding artery was possible with closure of the sole feeding artery (Fig. 3). Resection was then performed. Dedicated suture of medulla and cortex was performed as previously described [21]. The bulldog clamp/clamps was/were removed at the end of the renal parenchyma reconstruction.

2.3. Measurements

For each patient, we prospectively collected demographic data including age, body mass index and comorbidities classified according to the Charlson's comorbidity index [22], and clinical tumor size, side, location, and complexity according to the PADUA score [23]; perioperative data (including management of the renal pedicle, type and duration of ischemia: specifically for the purpose of this study, at the end of the procedure we evaluated the eventual success of the preoperatively planned management of renal pedicle); pathological data (including stage according to TNM [24]); and postoperative complications as classified according to the Clavien system [25]. Patients with a final diagnosis of renal cell carcinoma underwent oncological follow-up that consisted of history, physical examination, and an abdominal evaluation using ultrasound or CT scan on the basis of disease malignancy. Elective bone scan, chest CT, and magnetic resonance imaging (MRI) were performed when clinically indicated.

2.4. Image acquisition: CT contrast material injection and scan protocols

A CT scanner (Brilliance 64 slices; Philips Medical Systems, Best, The Netherlands) with a 64 × 0.625 detector configuration was used, with the following settings: rotation time, 0.75 s; section thickness and intersection gap, 0.7 mm and 0.3, respectively; helical pitch, 0.609; scan field of view, 50 cm; x-ray tube voltage, 120 kV; and x-ray tube current, 300 mA. All patients were administered nonionic iodine contrast material containing 350 mg I/ml (Iomeron; Bracco Imaging Italia srl) or 370 mg I/ml (Ultravist; Bayer Spa) using a double-syringe power injector (Stellant D; MedRad, Pittsburgh, PA, USA) at a rate of 4 ml/s through an at least 20-gauge angiocatheter placed in an antecubital vein. A bolus-tracking program was used to monitor the contrast enhancement after the injection of contrast medium before starting the diagnostic scans. Different scan delays for the three phases (arterial, nephrographic, and delayed phases) were set at 7 s, 70 s, and at least 10 min, respectively.

2.5. HA3D model rendering

Images in DICOM format were processed by M3DICS using dedicated software. The process consisted of the rendering of a 3D virtual model of the affected kidney, on the basis of high-resolution CT scans. HA3D was jointly performed by an experienced urologist and a professional engineer. It was focused on the renal vasculature (both arterial and venous), collecting system, kidney shape, and tumor characteristics. The renal pedicle and the tumor feeding arteries were reconstructed using the dynamic region growing method. Specifically for the purpose of this study, the course of the extra- and the intrarenal arteries was reconstructed till the segmental arteries (Fig. 4).

The renal parenchyma was segmented using selective thresholding, separating different voxels and grouping them according to the gray scale. Then, the virtual models were reviewed by bioengineers and urologists together, in order to evaluate the accuracy of the models in comparison with the obtained images. The next step was the creation of the mathematical HA3D model and the relative interactive 3D-PDF allowing for the navigation. The 3D-PDF file was viewed at every preoperative surgical planning stage and intraoperatively, with a dedicated assistant who navigated the model next to the first surgeon sitting at the robotic console.

2.6. Statistical analysis

Means and standard deviations were used to report continuous variables, and frequencies and proportions were used for categorical variables. Mean values for continuous variables were compared using the Student t test. The chi-square test was used for frequencies and proportions. A p value of <0.05 was considered statistically significant. Statistical analysis was performed by STATISTIC 7 (Statsoft Inc., Tulsa, OK, USA).

3. Results

Fifty-two patients who were diagnosed with a challenging renal mass (PADUA score >10) underwent RAPN during the enrollment phase. Among them, 31 patients treated until January 2016

underwent conventional bidimensional CT scan and represented "group no HA3D"; since February 2017, 21 patients underwent a high-resolution CT scan according to the abovementioned protocol with HA3D reconstruction and represented group HA3D. Patient demographics and preoperative characteristics are reported in Table 1. Median (standard deviation) tumor size was 50.9 (15.1) and 50.8 (16.1) mm ($p = 0.97$), and median (interquartile range) PADUA score 10.5 (10–11) and 11 (10–11; $p = 0.85$) for groups no HA3D and HA3D, respectively. Perioperative variables are reported in Table 2. In group no HA3D, a significantly higher rate of patients underwent global ischemia (80.6% vs 23.8%, $p < 0.01$), with 43% of patients in group HA3D receiving selective clamping of secondary-order arterial branches of the renal artery ($p < 0.01$). Of note, in 90.5% of the group HA3D cases, intraoperative management of the renal pedicle was done as preoperatively planned; in 38.7% of the group no HA3D cases, management of the renal arterial pedicle was intraoperatively varied ($p = 0.04$). A lower rate of opening of the collecting system was recorded in group HA3D (41.9 vs 14.3, group no HA3D vs group HA3D, $p = 0.05$). Moreover, no conversions to radical nephrectomy occurred (one occurred in group no HA3D, $p = 0.84$). No differences were found in functional outcomes (Table 3). Pathological data are reported in Table 4. One positive surgical margin was reported in group no HA3D.

4. Discussion

An issue of PN is the renal ischemia [5]. In almost all the cases of PN, global ischemia is performed even when it would not be required [14]. In such cases, arterial flow to the renal remnant is stopped with potential renal damage [6–8]. With the purpose of eliminating such damage, nonglobal ischemia techniques have been proposed [11], but remained of limited diffusion till the pure laparoscopic era, due to the technically demanding dissection of the renal pedicle with the pure laparoscopic approach [16]. Since the advent of robotics, a more precise surgery that allowed meticulous dissection of higher-order renal arterial branches was made possible [11,25]. The issue is that we cannot find/avoid what we are unable to see. Indeed, conventional CT prevents the whole

knowledge of the location of the lesion and its relationships with the renal vasculature. Some attempts have been made with 3D CT reconstruction techniques, typically presenting three structures (kidney, tumor, and renal vessels) [17,18,26]. With these techniques, the 3D reconstructed images were opaque, allowing adequate visualization of the extrarenal vasculature only.

This is why the surgeon's understanding of the relevant intrarenal anatomy during PN has remained wholly based on anatomical studies and preoperative CT-scan images combined with intraoperative visualization [9,10]. Mental elaboration by the surgeon in real time is required to merge the information deriving from all these elements.

In this setting, fluorescence guidance has been introduced, with the aim of helping selective clamping, but with limited diffusion, being empirical with a high percentage of failure [11−13]. Navigation technologies addressed to this issue seemed to be the right way: indeed Ukimura and Gill [17] proposed a 3D video representation of the opaque tumor and opaque extra- and intrarenal arterial tree in the setting of a semitransparent surface-rendered kidney. Thanks to the fact that the kidney itself was rendered semitransparent, visualization of intrarenal vasculature was possible. This technique was presented as allowing precise anatomical vascular microdissection with the goal of sponsoring the zero-ischemia PN, even in case of intrarenal tumors. After promising preliminary experience [19], we tried to improve the quality of the 3D reconstruction using dedicated software. Thanks to the specific protocol for images acquisition, HA3D reconstruction was obtained. The arterial vasculature was faithfully reproduced, allowing accurate dissection along the branches of the renal artery until the segmental arteries contacting the tumor surface. Indeed, the subjective concordance between the rendered images and the in vivo anatomy was satisfactory. The surgeon was able to simulate the selective ischemia caused by the different possibilities of selective clamping. In almost all the cases where we used this technique, global renal ischemia was avoided. Of note, in 90% of the patients who underwent RAPN with the novel technology, intraoperative management of the renal artery was performed as preoperatively planned, with all the selective

clampings being successful.

A proof of this was the almost bloodless renal tumor resection in all the cases, thus indicating a successful choice of the branches of the renal artery to be selectively clamped.

This kind of selective tumor-specific vascular control offered the considerable (although still debated) benefit of eliminating global renal ischemic injury during PN, even in a cohort of patients with anatomically complex tumors; such an advantage was of paramount importance in patients who had relative/imperative indications to PN, allowing for the preservation of the renal unit. In the presented cohort of patients, near-infrared fluorescence guidance was used. With the HA3D reconstruction, near-infrared fluorescence became the proof of the correct selective clamping rather than the tool that other authors and we are using to check if an empirically performed selective clamping is correct. Indeed, in our case series, successful selective clamping was corroborated by both the fluorescence and the bloodless resection bed during PN (Fig. 5).

After the era of the cognitive dissection of the renal pedicle, we integrated the HA3D reconstruction inside the console by Tile-Pro (Fig. 6). The efficacy of the superimposed imaging as guidance for the selective clamping was comparable with that of the cognitive guidance, with the advantage for the surgeon to remain focused on the operative field.

This study is not devoid of limitations. First, this is the initiation of a new technology and the sample size is limited. Second, the used segmentation technique may not be readily adaptable to MRI scans in patients who have contraindications to contrast-enhanced CT scan. Our segmentation technique required highly detailed thin-slice CT cuts of 0.5–1.0 mm thickness. As MRI scanning takes longer to perform than CT scanning, current MRI scans may not be able to provide such thin (<1 mm) multislice scanning during the patient's short breath-holding period.

Third, in the present study, the reconstructed images integrated inside the robotic console had to be moved according to the in vivo anatomy to have the overlapping of the virtual and the in vivo image.

Fourth, even if selective clamping was successful in the majority of cases, we acknowledge that

some cases had greater ischemia interval. If selective ischemia could theoretically be beneficial, a large body of data support that short duration of ischemia decreases the risk of permanent loss of renal function.

Notwithstanding these limitations, this study was more than satisfactory, with high concordance at overlapping of the 3D rendered virtual images and the in vivo anatomy. The indications to PN were expanded, with saved renal units even in patients who had imperative indications. Moreover, it allowed an increased rate of simple enucleation performed, representing a step in the right direction for the preservation of renal parenchyma. The most important aspect was the high accuracy of the preoperative planning and ischemia simulation with respect to the intraoperative setting.

The future perspective is the integration of the reconstructed images inside the robotic console. This is nowadays reality in our department, and we are living a pioneer experience that we sincerely hope to become a future publication.

5. Conclusions

HA3D virtual navigation technique allowed for a faithful representation of the kidney arterial vasculature. Preoperative simulation of selective ischemia was feasible and effective. In all the cases performed, selective clamping was successful, avoiding the ischemia of the healthy renal remnant. With this technology, fluorescence guidance becomes a double check of the correct planning of the selective clamping. Strict collaboration between urologists and bioengineers is required to achieve an automatized model, consolidated to the organ during the surgery.

References

[1] Maurice MJ, Ramirez D, Malkoç E, et al. Predictors of excisional volume loss in partial nephrectomy: is there still room for improvement? Eur Urol 2016;70:413–5.

[2] Simmons MN1, Hillyer SP, Lee BH, Fergany AF, Kaouk J, Campbell SC. Functional recovery after partial nephrectomy: effects of volume loss and ischemic injury. J Urol 2012;187:1667–73.

[3] Marconi L, Desai MM, Ficarra V, Porpiglia F, Van Poppel H. Renal preservation and partial nephrectomy: patient and surgical factors. Eur Urol Focus 2016;2:589–600.

[4] Porpiglia F, Bertolo R, Fiori C. Words of wisdom: Re: Residual parenchymal volume, not warm ischemia time, predicts ultimate renal functional outcomes in patients undergoing partial nephrectomy. Eur Urol 2016;69:176–7.

[5] Volpe A, Blute ML, Ficarra V, et al. Renal ischemia and function after partial nephrectomy: a collaborative review of the literature. Eur Urol 2015;68:61–74.

[6] Rod X, Peyronnet B, Seisen T, et al. Impact of ischaemia time on renal function after partial nephrectomy: a systematic review. BJU Int 2016;118:692–705.

[7] Rocca Rossetti S. Impact of acute ischemia in human kidney. In: Marberger M, Dreikon A, editors. Renal preservation. London, UK: Baltimore; 1983. p. 21–37.

[8] Porpiglia F, Bertolo R, Amparore D, et al. Evaluation of functional outcomes after laparoscopic partial nephrectomy using renal scintigraphy: clamped vs clampless technique. BJU Int

2015;115:606–12.

[9] GravesFT. The anatomy of the intrarenal arteries and its application to segmental resection of the kidney. Br J Surg 1954;42:132–9.

[10] Macchi V, Crestani A, Porzionato A, et al. Anatomical study of renal arterial vasculature and its potential impact on partial nephrectomy. BJU Int 2017;120:83–91.

[11] Simone G, Gill IS, Mottrie A, et al. Indications, techniques, outcomes, and limitations for minimally ischemic and off-clamp partial nephrectomy: a systematic review of the literature. Eur Urol 2015;68:632–40.

[12] Komninos C, Shin TY, Tuliao P, et al. Renal function is the same 6 months after robot-assisted partial nephrectomy regardless of clamp technique: analysis of outcomes for off-clamp, selective arterial clamp and main artery clamp techniques, with a minimum follow-up of 1 year. BJU Int 2015;115:921–8.

[13] Desai MM, de Castro Abreu AL, Leslie S, et al. Robotic partial nephrectomy with superselective versus main artery clamping: a retrospective comparison. Eur Urol 2014;66:713–9.

[14] Lieberman L, Barod R, Dalela D, et al. Use of main renal artery clamping predominates over minimal clamping techniques during robotic partial nephrectomy for complex tumors. J Endourol 2017;31:149–52.

[15] Autorino R, Porpiglia F, Dasgupta P, et al. Precision surgery and genitourinary cancers. Eur J Surg Oncol 2017;43:893–908.

[16] Porpiglia F, Fiori C, Checcucci E, Pecoraro A, Di Dio M, Bertolo R. Selective clamping during laparoscopic partial nefrectomy: the use of near infrared fluorescence guidance. Minerva Urol Nefrol. In press. http://dx.doi.org/10.23736/S0393-2249.17.03046-6

[17] Ukimura O, Gill IS. Imaging-assisted endoscopic surgery: Cleveland Clinic experience. J Endourol 2008;22:803–10.

[18] Shao P, Tang L, Li P, et al. Application of a vasculature model and standardization of the renal hilar approach in laparoscopic partial nephrectomy for precise segmental artery clamping. Eur Urol

2013;63:1072–81.

[19] Porpiglia F, Bertolo R, Checcucci E, et al. Development and validation of 3D printed virtual models for robot-assisted radical prostatectomy and partial nephrectomy: urologists' and patients' perception. World J Urol. In press. http://dx.doi.org/10.1007/s00345-017-2126-1

[20] Levey AS, Bosch JP, Lewis JB, Greene T, Rogers N, Roth D. A more accurate method to estimate glomerular filtration rate from serum creatinine: a new prediction equation. Modification of Diet in Renal Disease Study Group. Ann Intern Med 1999;130:461–70.

[21] Porpiglia F, Bertolo R, Amparore D, Fiori C. Nephron-sparing suture of renal parenchyma after partial nephrectomy: which technique to go for? Some best practices. Eur Urol Focus. In press. http://dx.doi.org/10.1016/j.euf.2017.08.006

[22] Nuttalla M, van der Meulena J, Embertona M. Charlson scores based on ICD-10 administrative data were valid in assessing comorbidity in patients undergoing urological cancer surgery. J Clin Epidemiol 2006;59:265–73.

[23] Ficarra V, Novara G, Secco S, et al. Preoperative aspects and dimensions used for an anatomical (PADUA) classification of renal tumours in patients who are candidates for nephron-sparing surgery. Eur Urol 2009;56:786–93.

[25] Moch H, Artibani W, Delahunt B, et al. Reassessing the current UICC/AJCC TNM staging for renal cell carcinoma. Eur Urol 2009;56:636–43.

[24] Dindo D, Demartines N, Clavien PA. Classification of surgical complications: a new proposal with evaluation in a cohort of 6336 patients and results of a survey. Ann Surg 2004;240:205–10.

[25] Satkunasivam R, Tsai S, Syan S, et al. Robotic unclamped "minimal-margin" partial nephrectomy: ongoing refinement of the anatomic zero-ischemia concept. Eur Urol 2015;68:705–12.

[26] Bertolo R, Zargar H, Autorino R, et al. Estimated glomerular filtration rate, renal scan and volumetric assessment of the kidney before and after partial nephrectomy: a review of the current literature. Minerva Urol Nefrol 2017;69:539–47.

Fig. 1 – Simulation on the created hyperaccuracy 3D reconstruction for the management of the renal pedicle and the subsequent ischemia.

Fig. 2 – Dissection of the renal pedicle guided by the hyperaccuracy 3D reconstruction: (A) standard anatomy; (B) computer-made superimposed imaging. The reconstruction is available on the tablet next to the console, manually oriented by the assistant, according to the in vivo anatomy. From the main artery, dissection is carried on following the renal arterial branches as anticipated by the virtual model, till the identification of the arterial branch/branches supplying the tumor.

Fig. 3 – Complex renal pedicle dissection aided by the hyperaccuracy 3D reconstruction: (A) isolation of the renal arterial branches is completed by using vessel loops; (B) tumor dedicated feeding artery is identified (*).

Fig. 4 – Hyperaccuracy 3D reconstruction: (A) axial view; (B) coronal view). The renal pedicle and the tumor feeding arteries are reconstructed using the dynamic region growing method. The course of the extra- and the intraparenchymal arteries is reconstructed till the segmental arteries contacting the tumor surface.

Fig. 5 – (A) Near-infrared fluorescence performed after (B) selective clamping based on the hyperaccuracy 3D reconstruction. The successful selective clamping is proved by fluorescence, showing the selective devascularization of the tumor as anticipated by the virtual model.

Fig. 6 – (A) Hyperaccuracy 3D reconstruction is integrated inside the console by Tile-Pro. (B) Intraoperative ultrasonography is paired to the superimposed imaging to identify the completely intrarenal tumor.

Table 1 – Patient demographics and preoperative characteristics

	No HA3D	HA3D	*p* value
No. of patients	31	21	
No. of males (%)	23 (74.2)	15 (71.4)	0.92
Age (yr), mean (SD)	59.5 (10.6)	60.8 (12.3)	0.66
BMI (kg/m^2), median (IQR)	25 (23.5; 25)	24 (23.5; 25.5)	0.24
CCI, median (IQR)	0 (0; 1)	1 (0; 2)	0.32
Age-adjusted CCI, median (IQR)	3 (2; 4)	2 (2; 3)	0.14
ECOG, median (IQR)	0 (0; 1)	0 (0; 1)	0.74
ASA score, median (IQR)	2 (1; 2)	1 (1; 1)	0.06
Preoperative hemoglobin (mg/dl), mean (SD)	14.4 (1.6)	13.5 (2.4)	0.11
No. of solitary kidneys (%)	2 (6.4)	1 (4.8)	0.91
Tumor size at CT scan (mm), mean (SD)	50.9 (15.1)	50.8 (16.1)	0.97
No. of right-sided tumors (%)	16 (51.6)	10 (47.6)	0.83
Clinical stage, no. (%)			
cT1a	10 (32.3)	4 (19.0)	0.46
cT1b	16 (51.6)	11 (52.4)	0.81
≥cT2	5 (16.1)	6 (28.56)	0.46
PADUA score, median (IQR)	10.5 (10; 11)	11 (10; 11)	0.85
Tumor location (up/low), no. (%)			
Upper pole	7 (22.5)	3 (14.3)	0.70
Mediorenal	11 (35.5)	9 (42.85)	0.80
Lower pole	13 (41.9)	9 (42.85)	0.82
Tumor location (ant/post), no. (%)			
Anterior	16 (51.6)	9 (42.9)	0.74
Posterior	15 (48.4)	12 (57.1)	0.73
Tumor location (rim), no. (%)			
Lateral rim	13 (41.9)	8 (38.1)	0.99
Medial rim	18 (58.1)	13 (61.9)	0.99
Tumor growth pattern, no. (%)			

≥50% Exophytic	4 (12.9)	4 (19.1)	0.83
<50% Exophytic	21 (67.7)	11 (52.3)	0.40
Endophytic	6 (19.4)	6 (28.6)	0.66
Indication to PN, no. (%)			
Elective	26 (83.9)	17 (80.9)	0.92
Relative	1 (3.2)	1 (4.8)	0.65
Imperative	4 (12.9)	3 (14.3)	0.78

ASA = American Society of Anesthesiologists; BMI = body mass index; CCI = Charlson's comorbidity index; CT = computed tomography; ECOG = Eastern Cooperative Oncology Group; HA3D = hyperaccuracy three-dimensional reconstruction; IQR: interquartile range; PN = partial nephrectomy; SD = standard deviation.

Table 2 – Perioperative variables

	No HA3D	HA3D	p value
No. of patients	31	21	
Resection technique, no. (%)			
Simple enucleation	9 (29.0)	11 (52.4)	0.15
Standard PN	22 (71.0)	10 (47.6)	0.15
Clamping of renal artery, no. (%)			
Global ischemia	25 (80.6)	5 (23.8)	<0.01
Selective of I order branch	1 (3.2)	2 (9.5)	0.72
Selective of II order branch	2 (6.5)	9 (42.9)	<0.01
Superselective of feeding arteries	1 (3.2)	3 (14.3)	0.34
Clampless	2 (6.5)	2 (9.5)	0.90
Management of renal pedicle as planned, no. (%)	19 (61.3)	19 (90.5)	0.04
Ischemia time (min), mean (SD)			
Global ischemia	24.9 (6.3)	26.3 (4.6)	0.41
Partial ischemia	20.1 (4.2)	21.5 (5.6)	0.29
EBL (ml), mean (SD)	129.0 (182.1)	131.6 (246.8)	0.96
Operative time (min), mean (SD)	123.3 (61.8)	131.1 (43.1)	0.61
Use of intraoperative US, no. (%)	19 (61.3)	13 (61.9)	0.80

No. of openings of the collecting system (%)	13 (41.9)	3 (14.3)	0.05
No. of intraoperative complications (%)	1 (3.2)	1 (4.8)	0.65
No. of transfusions (%)	1 (3.2)	1 (4.8)	0.65
No. of conversion to radical nephrectomy (%)	1 (3.2)	0 (0)	0.84
No. of postoperative complications, Clavien (%)			
<3	6 (19.3)	4 (19.0)	0.74
≥3	1 (3.2)	1 (4.8)	0.65

EBL = estimated blood loss; HA3D = hyperaccuracy three-dimensional reconstruction; PN = partial nephrectomy; SD = standard deviation; US = ultrasonography.

Table 3 – Functional variables

	No HA3D	HA3D	*p* value
No. of patients	31	21	
Preoperative SCr (mg/dl), mean (SD)	1.0 (0.3)	1.0 (0.4)	0.95
Preoperative eGFR (ml/min), mean (SD)	75.9 (22.4)	75.7 (23.3)	0.97
Postoperative SCr (mg/dl), mean (SD)	1.2 (0.4)	1.2 (0.5)	0.80
Postoperative eGFR (ml/min), mean (SD)	68.8 (26.2)	62.5 (23.4)	0.37
ΔSCr (mg/dl), mean (SD)	+15.4 (26.8)	+14.8 (25.9)	0.93
ΔeGFR (ml/min), mean (SD)	−12.0 (20.7)	−12.4 (20.1)	0.94
Preoperative %SRF, mean (SD)	51.6 (7.4)	48.1 (10.1)	0.07
Postoperative %SRF, mean (SD)	46.5 (8.9)	42.5 (13.2)	0.19
Preoperative ERPF, mean (SD)	185.7 (42.0)	174.9 (54.5)	0.09
Postoperative ERPF, mean (SD)	176.32 (29.70)	164.25 (57.25)	0.32
ΔSRF, mean (SD)	10.59 (8.01)	11.21 (8.63)	0.79
ΔERPF, mean (SD)	17.39 (10.77)	16.32 (11.24)	0.73

eGFR = estimated glomerular filtration rate; ERPF = effective renal plasmatic flow; HA3D = hyperaccuracy three-dimensional reconstruction; SCr = serum creatinine; SD = standard deviation; SRF = split renal function.

Table 4 – Final pathology results

	No HA3D	HA3D	*p* value
No. of patients	31	21	
Malignant, no. (%)	28 (90.3)	20 (95.2)	0.89
Pathological stage, no. (%)			
pT1a	6 (21.4)	3 (15.0)	0.81
pT1b	11 (39.3)	8 (40.0)	0.91
pT2	2 (7.1)	3 (15.0)	0.60
pT3	9 (32.2)	6 (30.0)	0.73
Tumor size at final pathology (mm), mean (SD)	49.8 (15.3)	50.2 (15.9)	0.92
No. of positive surgical margin (%)	1 (3.22)	0 (0)	0.84
Histology, no. (%)			
Clear cell carcinoma	23 (74.2)	18 (85.7)	0.56
Papillary	2 (6.45)	1 (4.76)	0.72
Cromophobe	2 (6.45)	1 (4.76)	0.72
Oncocytoma	0 (0)	1 (4.76)	0.84
Angiomyolipoma	0 (0)	0 (0)	–
Unclassified	3 (9.7)	0 (0)	0.38
Other	1 (3.2)	0 (0)	0.84
ISUP grade, no. (%)			
1	4 (14.3)	0 (0)	0.13
2	13 (45.4)	12 (60.0)	0.40
3	4 (14.3)	6 (30.0)	0.26
4	7 (25.0)	2 (10.0)	0.39

ISUP = International Society of Urological Pathology; SD = standard deviation.

Figure 1
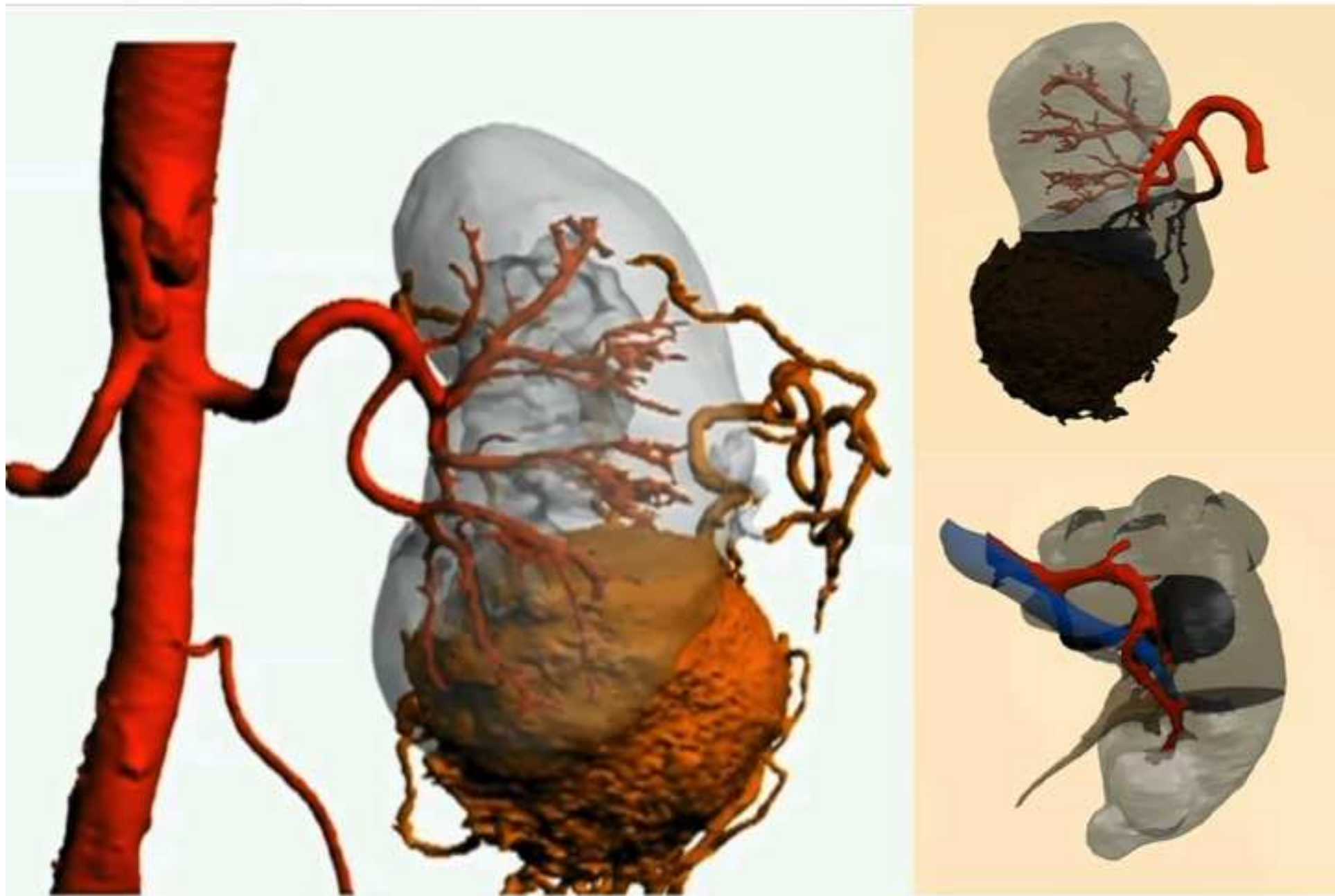**Click here to download high resolution image**

Figure 2
[Click here to download high resolution image](#)

Figure 3
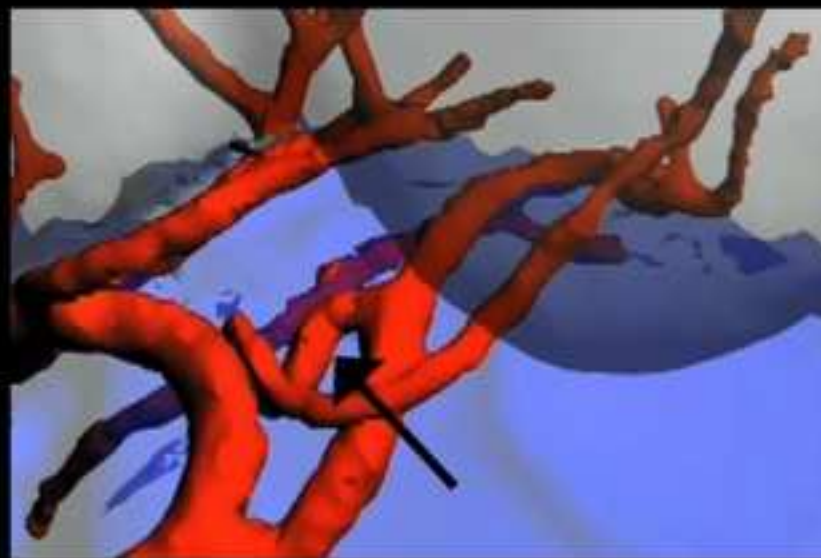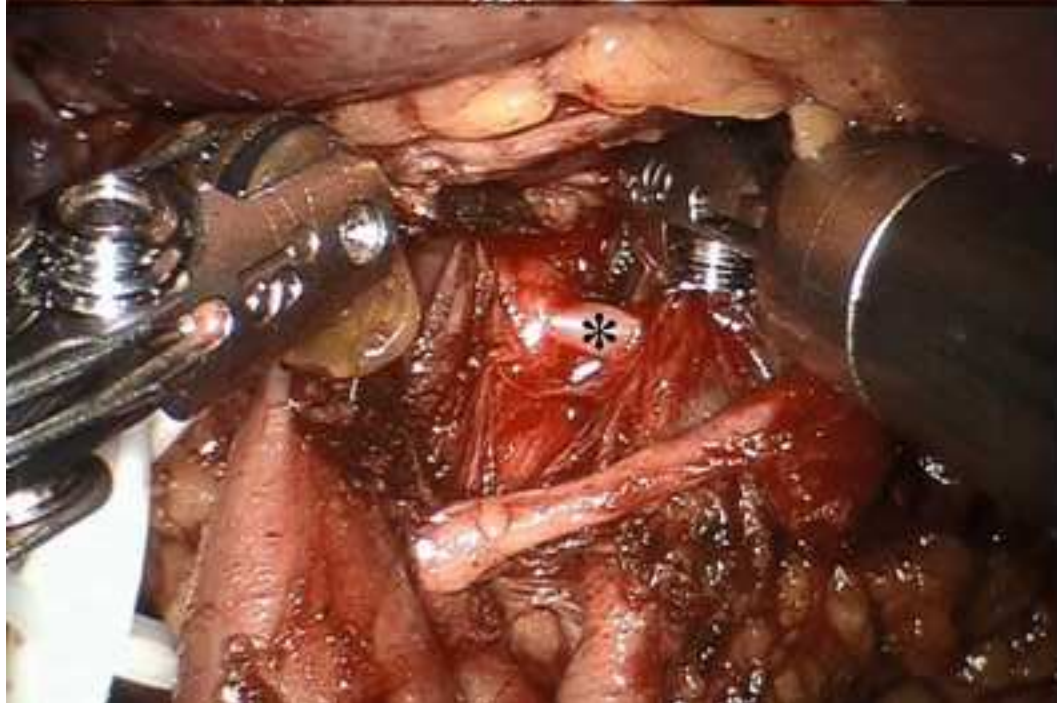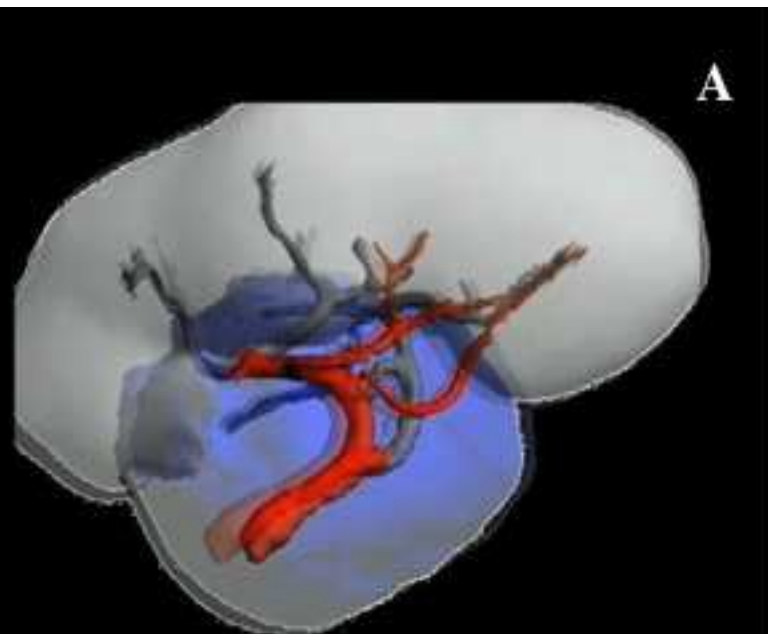[Click here to download high resolution image](#)

Figure 4
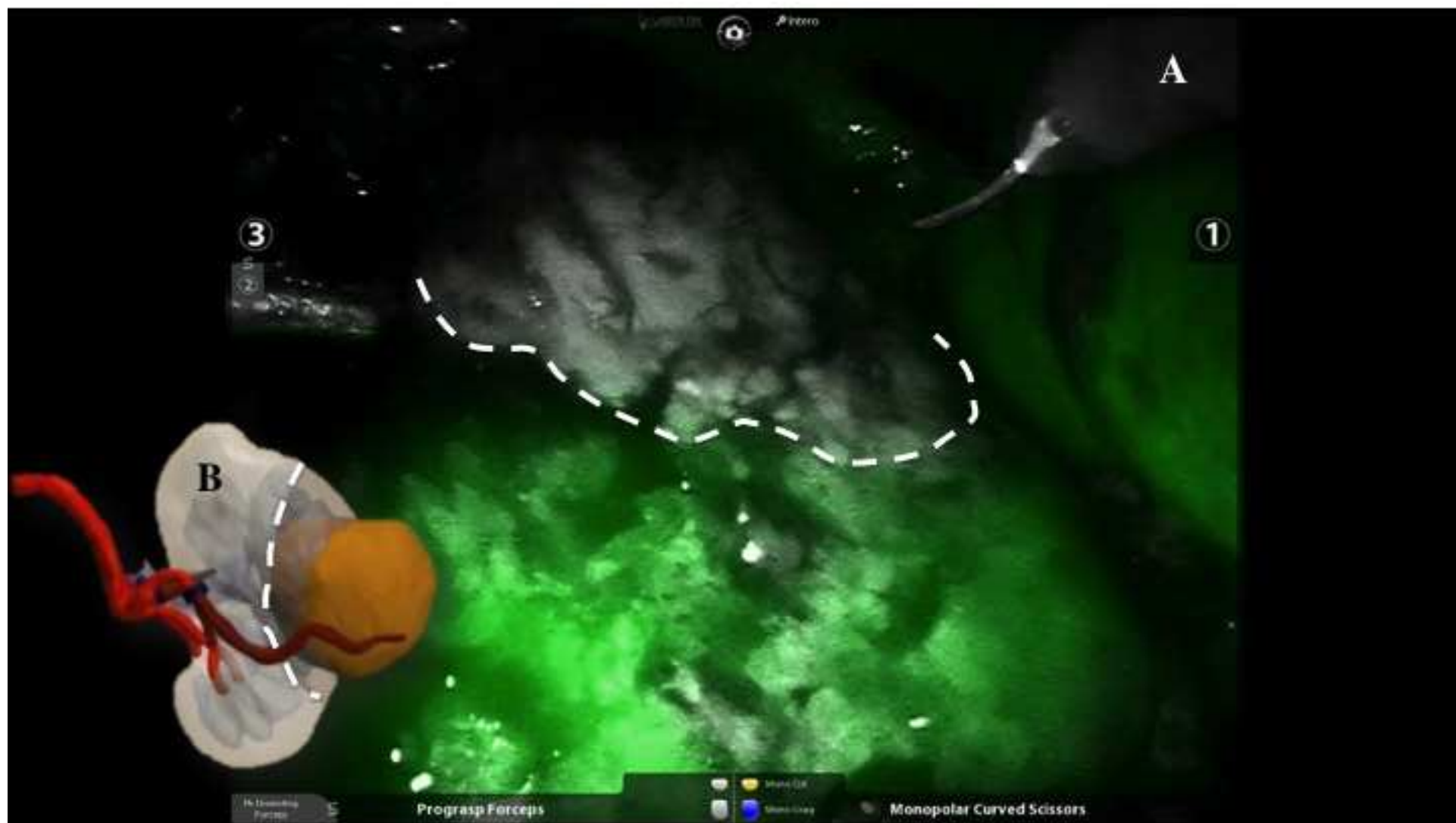[Click here to download high resolution image](#)

Figure 6
[Click here to download high resolution image](#)